

# Possible Triplet $p + ip$ Superconductivity in Graphene at Low Filling

Tianxing Ma,<sup>1,2</sup> Fan Yang,<sup>3,2,\*</sup> Hong Yao,<sup>4,5,†</sup> and Hai-Qing Lin<sup>2</sup>

<sup>1</sup>*Department of Physics, Beijing Normal University, Beijing 100875, China*

<sup>2</sup>*Beijing Computational Science Research Center, Beijing 100084, China*

<sup>3</sup>*School of Physics, Beijing Institute of Technology, Beijing, 100081, China*

<sup>4</sup>*Institute of Advanced Study, Tsinghua University, 100081, China*

<sup>5</sup>*Collaborative Innovation Center of Quantum Matter, Beijing, China*

We study the Hubbard model on the honeycomb lattice with nearest-neighbor hopping ( $t > 0$ ) and next-nearest-neighbor one ( $t' < 0$ ). When  $t' < -t/6$ , the single-particle spectrum is featured by the continuously distributed Van-Hove saddle points at the band bottom, where the density of states diverges in power-law. We investigate possible unconventional superconductivity in such system with Fermi level close to the band bottom by employing both random phase approximation and determinant quantum Monte-Carlo approaches. Our study reveals a possible triplet  $p + ip$  superconductivity in this system with appropriate interactions. Our results might provide a possible route to look for triplet superconductivity with relatively-high transition temperature in a low-filled graphene and other similar systems.

**Introduction:** Graphene, a single layer of carbon atoms forming a honeycomb lattice, has been among the most exciting research fields since synthesized[1]. Enormous attentions on this remarkable material have been focused on exploring physics related to its Dirac-cone band structure[2]. For graphene close to half-filling, the density of states (DOS) at the Fermi level is almost vanishing; as a consequence, relatively weak/intermediate short-range repulsive interactions in general do not induce phase transitions at low temperature[2]. Nonetheless, exotic phases might be induced by repulsive interactions when the Fermi level is finitely away from the Dirac point. For instance, it was shown by renormalization group (RG) calculations that unconventional/topological superconductivity (SC) is induced by weak repulsive interactions in honeycomb Hubbard models finitely away from half-filling[3]. More recently, exotic phases such as  $d + id$  [3–9] topological superconductivity[10, 11] and Chern band insulators with spin density waves[12, 13] near the type-I Van-Hove singularity (VHS) at  $1/4$  electron or hole doping, where the DOS at Fermi level diverges logarithmically. Such logarithmically diverging DOS close the VHS may significantly raise superconducting transition temperature. More recently, it was shown by RG analysis that topological triplet  $p + ip$  superconductivity can generically occur in systems at type-II VHS where the saddle points are not at time-reversal-invariant momenta[14, 15].

In 2D, for a Fermi surface with discrete Van-Hove saddle points, the DOS at Fermi level diverges only logarithmically. It would be interesting to study phases in systems with a power-law diverging DOS. Indeed, it was shown that for  $t' < -t/6$  an inverse-square-root diverging DOS occurs close to band bottom of the lower band, where the band bottom is a closed line instead of discrete points as shown in Fig. 1 (b). In low-filled graphene,  $t'$  is estimated to be about  $-0.2t$ [16]. Note that the band bottom occurring at a closed line only when

no third-neighbor or longer-range hopping is considered. This kind of line band bottom may be considered as a set of continuously distributed VH saddle points. Recent determinant quantum Monte-Carlo (DQMC) study has revealed ferromagnetic-like spin-correlations in such system[17], which implies possibility of a dominant triplet pairing state in this system with repulsive interactions.

In this paper, we report both random phase approximation (RPA) analysis and DQMC studies of pairing symmetries of possible SC induced by weak or intermediate repulsive interactions in graphene at low fillings whose DOS at Fermi level is significantly enhanced by the power-law singularity at the band bottom. Both numerical approaches obtain the  $p + ip$  triplet pairing as the leading instability of the system in different parameter regimes. For  $t' = -0.2t$ ,  $U/t = 3.0$ , and filling  $n = 0.2$ , the transition temperature  $T_{c,\text{triplet}}$  into the triplet pairing state is estimated to be in the order of  $10^{-2}t$ . For graphene  $t \sim 2.0\text{eV}$ , this implies that the  $T_{c,\text{triplet}}$  in graphene might be as high as 200K when the Fermi level is tuned appropriately close to the band bottom. These results might provide a possible route to look for triplet superconductivity with relatively-high transition temperature in graphene at low filling.

**Model:** We start from the following Hubbard model on the honeycomb lattice

$$H = -t \sum_{\langle i,j \rangle} c_{i\sigma}^\dagger c_{j\sigma} - t' \sum_{\langle\langle i,j \rangle\rangle} c_{i\sigma}^\dagger c_{j\sigma} + U \sum_i n_{i\uparrow} n_{i\downarrow}, \quad (1)$$

where  $c_{i\sigma}^\dagger$  is the electron creation operator at site  $i$  and with spin polarization  $\sigma = \uparrow, \downarrow$  and  $U$  labels the on-site repulsive interaction. Here the  $t$  and  $t'$  terms describe the nearest neighbor (NN) and next nearest neighbor (NNN) hoppings, respectively. We focus on the case of  $t > 0$  and  $t' < 0$  with  $t' < -t/6$ , relevant to graphene. Hereafter, we adopt  $t' = -0.2t$  in our calculations unless stated otherwise. The resulting band structure is shown in Fig. 1(a), together with the Fermi levels for filling  $n = 0.2$

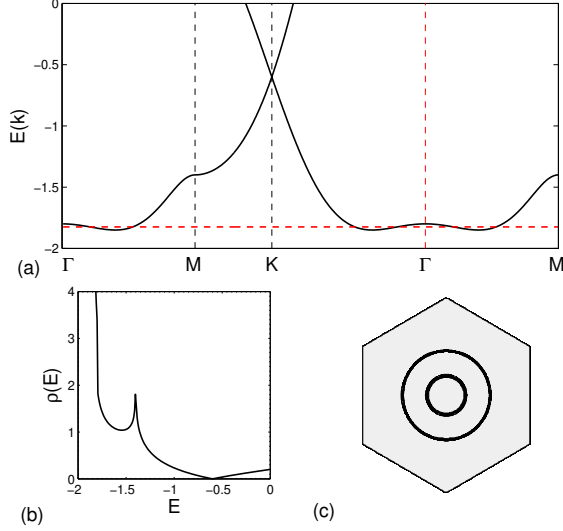


FIG. 1. (Color online) (a) The energy band along high symmetry line in the first Brillouin Zone; (b) The DOS as function of energy with  $t' = -0.2t$ ; and (c) The Fermi surface at filling  $n = 0.2$ .

per site. We notice one remarkable feature of this band structure: the band bottom of this system does not locate at the  $\Gamma$ -point; instead it consists two closed lines around  $\Gamma$ . As a consequence, the DOS is divergent in an inverse-square-root fashion near the band bottom, as shown in Fig. 1(b). The Fermi surface (FS) of the system at  $n = 0.2$  is shown in Fig. 1(c), which contains an inner hole-pocket and an outer electron-pocket. In the following, we adopt perturbative RPA analysis for weak  $U$  interactions and the DQMC calculations for relatively strong  $U$  to investigate the pairing symmetries of the possible SC at low filling.

**RPA treatment:** We adopted the standard multi-orbital RPA approach[18–23] in our study for the small  $U$  ( $= 0.1t$ ) case. Various susceptibilities of non-interacting electrons of this system are defined as

$$\chi_{l_3, l_4}^{(0)l_1, l_2}(\mathbf{q}, \tau) \equiv \frac{1}{N} \sum_{\mathbf{k}_1, \mathbf{k}_2} \left\langle T_\tau c_{l_1}^\dagger(\mathbf{k}_1, \tau) c_{l_2}(\mathbf{k}_1 + \mathbf{q}, \tau) c_{l_3}^\dagger(\mathbf{k}_2 + \mathbf{q}, 0) c_{l_4}(\mathbf{k}_2, 0) \right\rangle_0 \quad (2)$$

where  $l_i$  ( $i = 1, 2$ ) denotes orbital (sublattice) index. Largest eigenvalues of the susceptibility matrix  $\chi_{l, m}^{(0)}(\mathbf{q}) \equiv \chi_{m, m}^{(0)l, l}(\mathbf{q}, i\nu = 0)$  is shown in Fig. 2 for filling  $n = 0.1$ , which shows dominant distributions on a small circle around the  $\Gamma$ -point. This suggests strong ferromagnetic-like intra-sublattice spin fluctuations in the system. Generally, it is found that at low fillings, the radius of the circle scales with filling. At low fillings, the eigenvector of the susceptibility matrix reveals that the inter-sublattice spin fluctuations in the system are also ferromagnetic-like, although somewhat weaker than

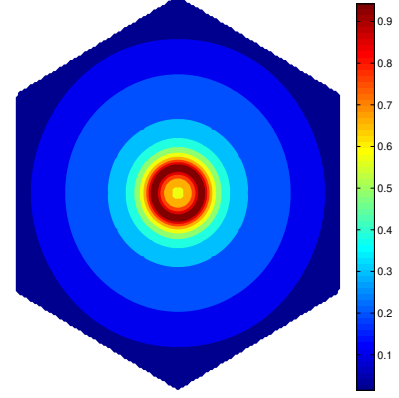


FIG. 2. (Color online) Largest eigenvalues of the susceptibility matrix in non-interacting limit in the first Brillouin-Zone.

the intra-sublattice ones. Such ferromagnetic-like spin fluctuations are consistent with the ferromagnetic spin correlations revealed by the DQMC calculations[17].

With finite but weak Hubbard interactions  $U$ , the spin ( $\chi^s$ ) or charge ( $\chi^c$ ) susceptibilities in the RPA level are given by

$$\chi^{s(c)}(\mathbf{q}, i\nu) = \left[ I \mp \chi^{(0)}(\mathbf{q}, i\nu) \bar{U} \right]^{-1} \chi^{(0)}(\mathbf{q}, i\nu), \quad (3)$$

where  $\bar{U}_{\mu\nu}^{\mu\nu}$  ( $\mu\nu = 1, 2$ ) is a  $4 \times 4$  matrix, whose only two nonzero elements are  $\bar{U}_{11}^{11} = \bar{U}_{22}^{22} = U$ . It's clear that the repulsive Hubbard-interaction suppresses  $\chi^c$  but enhances  $\chi^s$ . Thus, the spin fluctuations take the main role of mediating the cooper pairing in the interacting system[18]. In the RPA level, the cooper pairs near the FS acquire an effective interaction  $V_{\text{eff}}$ [18, 19, 23] via exchanging the spin fluctuations represented by the renormalized spin susceptibilities. From this effective interaction, one obtains the linearized gap equation near the superconducting critical temperature  $T_c$ , solving which one obtains the leading pairing symmetry (symmetries) of the system.

Our results for  $n=0.1$  and  $n=0.2$  reveal that the leading pairing symmetries of the system at these low fillings are degenerate  $p_x$  and  $p_y$  doublets, as shown in Fig. 3(a) and (b), which should be further mixed as  $p_x \pm ip_y$  to minimize the ground state energy, as suggested by our further mean-field calculations on the effective Hamiltonian. Such a triplet pairing is mediated by the ferromagnetic-like spin fluctuations in the system, as shown in Fig. 2. The subleading pairing symmetries of the system at these low fillings are also obtained, which are triplet  $f$ -wave shown in Fig. 4(a) for  $n = 0.1$  and singlet  $d_{xy}$  and  $d_{x^2-y^2}$  doublets (which should further be mixed as  $d_{xy} \pm id_{x^2-y^2}$  to lower the energy), as shown in Fig. 5(a) and (b) for  $n = 0.2$ .

Note that we have chosen such a small  $U$  as  $U = 0.1t$

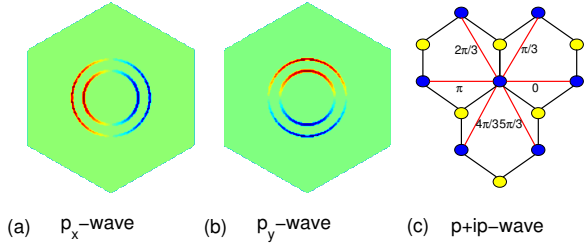


FIG. 3. (Color online) (a) and (b) show the  $p_x$  and  $p_y$  pairing symmetries in the  $k$ -space and (c) shows the phase of the  $p+ip$  pairing symmetry on the honeycomb lattice in the real space.

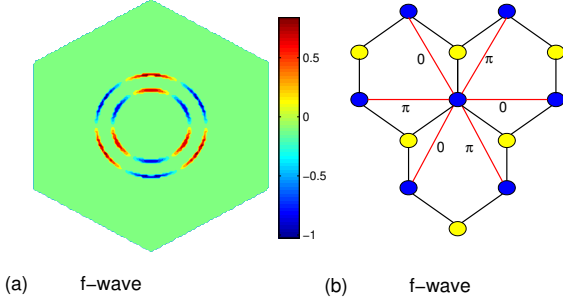


FIG. 4. (a) shows the  $f$  pairing in the  $k$ -space and (b) shows the phase of the  $f$  pairing symmetries in the real space.

in our RPA calculations. For larger  $U$  beyond its critical value  $U_c$ , the divergence of the spin susceptibility invalidate our RPA calculations for superconductivity. Physically, such a divergent spin susceptibility for  $U > U_c$  may not necessarily lead to a magnetically-ordered state since the distribution of the susceptibility shown in Fig. 2 does not possess a sharply peaked structure at particular momentum. Instead, the competition among different wave vectors may lead to paramagnetic behavior or short-ranged spin correlations which provide basis for the cooper pairing. We leave the study for the case of  $U > U_c$  to the following DQMC approach, which is suitable for strong coupling problems.

**DQMC simulations:** The DQMC simulation is a

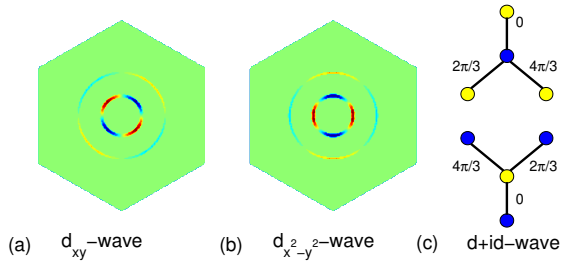


FIG. 5. (Color online) (a) and (b) show the  $d_{xy}$  and  $d_{x^2-y^2}$  pairing symmetries in the  $k$ -space and (c) shows the phase of the  $d+id$  pairing symmetries in the real space.

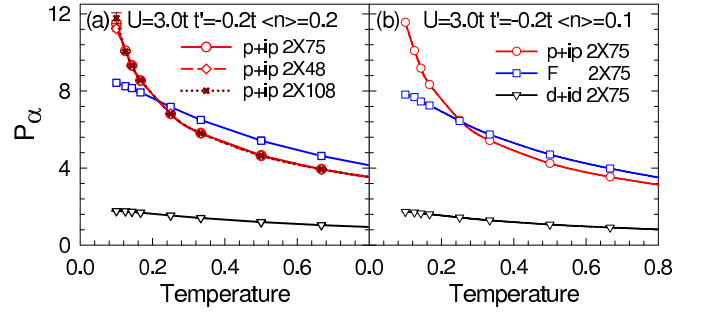


FIG. 6. (Color online) Pairing susceptibility  $P_\alpha$  as a function of temperature for different pairing symmetries with  $U = 3t$  at  $\langle n \rangle = 0.2$  (a) and  $\langle n \rangle = 0.1$  (b) on a  $2 \times 75$  lattice (solid line). The  $P_{p+ip}$  at  $\langle n \rangle = 0.2$  on a  $2 \times 48$  lattice (dash red line) and a  $2 \times 108$  lattice are also shown (dotted red line) in (a). Here the units of temperature is  $t$ .

powerful unbiased numerical tool to study the physical properties of such strongly-correlated electronic systems as the Hubbard model. The basic strategy of DQMC is to express the partition function as a high-dimensional integral over a set of random auxiliary fields. The integral is then accomplished by Monte Carlo techniques. In most of our simulations, 10000 sweeps were used to equilibrate the system. An additional 40000 sweeps were then made, each of which generated a measurement. These measurements were split into twenty bins which provide the basis of coarse-grain averages and errors were estimated based on standard deviations from the average. For more technique details, we refer to Refs. [17, 24, 25].

To investigate the SC property within the DQMC approach, we compute the pairing susceptibility,

$$P_\alpha \equiv \frac{1}{N_s} \sum_{i,j} \int_0^\beta d\tau \langle \Delta_\alpha^\dagger(i, \tau) \Delta_\alpha(j, 0) \rangle. \quad (4)$$

Here  $\alpha$  stands for the pairing symmetry, and the corresponding pairing order parameter  $\Delta_\alpha^\dagger(i)$  is defined as

$$\Delta_\alpha^\dagger(i) \equiv \sum_l f_\alpha^*(\delta_l) (c_{i\uparrow} c_{i+\delta_l\downarrow} \pm c_{i\downarrow} c_{i+\delta_l\uparrow})^\dagger, \quad (5)$$

where  $f_\alpha(\delta_l)$  is the form factor of the pairing function, the vectors  $\delta_l$  denote the bond connections, and “ $\pm$ ” labels triplet/singlet symmetries respectively.

Guided by the RPA results, three different pairing symmetries were investigated in the following DQMC studies, *i.e.*  $p+ip$ ,  $f$ , and  $d+id$  symmetries, whose form factors are illustrated in Fig. 3(c), Fig. 4(b), and Fig. 5(b) respectively. These different pairing symmetries can be distinguished by their different phase shifts upon each  $60^\circ$  rotation, which are  $\pi/3$ ,  $2\pi/3$  and  $\pi$  respectively. The NNN-bond  $p+ip$  and  $f$  wave triplet pairings shown possess the following form factors,

$$f_{p+ip}(\delta_l) = e^{i(l-1)\frac{\pi}{3}}, \quad f_f(\delta_l) = (-1)^l, \quad l = 1, \dots, 6, \quad (6)$$

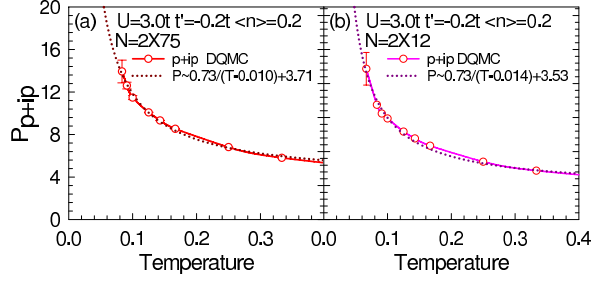


FIG. 7. (Color online) Pairing susceptibility  $P_{p+ip}$  as a function of temperature with  $U = 3t$  and  $\langle n \rangle=0.2$  for a  $2 \times 75$  lattice (a) and a  $2 \times 12$  lattice (b) (solid line). The fitting data are also shown as dashed lines.

and the NN-bond singlet  $d + id$  pairing shown possesses the form factor

$$f_{d+id}(\delta_l) = e^{i(l-1)\frac{2\pi}{3}}, \quad l = 1, 2, 3. \quad (7)$$

Note that the NN-bond pairing is prohibited in the  $f$ -wave symmetry. As for the  $p + ip$  and  $d + id$  symmetries, although both the NN-bond and the NNN-bond pairings are allowed, our DQMC calculations show stronger NNN-bond pairings for the  $p + ip$  symmetry while stronger NN-bond pairings for the  $d + id$  one, reflecting the fact that the spin-fluctuations on the NNN-bond are more ferromagnetic-like than those on the NN-bond, consistent with our RPA calculations. We have also studied longer-range pairings by adding third and forth bond pairings in former factors, which turn out be much weaker than that of the NN-bond and NNN-bond pairings presented above.

Our DQMC simulations of the system were performed at finite temperatures on a  $2 \times 48$ , a  $2 \times 75$  and a  $2 \times 108$  lattices with periodic boundary conditions. Fig. 6 shows the temperature dependence of the pairing susceptibilities for different pairing symmetries with electron filling  $n=0.2$  (a) and  $n=0.1$  (b) with  $U = 3t$ . Within the parameter range investigated, the pairing susceptibilities for various pairing symmetries increase as the temperature is lowered, and most remarkably, the  $p + ip$  pairing symmetry dominates other pairing symmetries at relatively low temperatures, consistent with the RPA results. In Fig. 6 (a), the pairing susceptibility  $P_{p+ip}$  on a  $2 \times 48$  and a  $2 \times 108$  lattices are also shown, in comparison with that on the  $2 \times 75$  lattice, from which one verifies negligible finite size effects.

The superconducting transition occurs as the pairing susceptibility diverges. However, DQMC simulations encounter the notorious minus problem in this doped system as well; consequently the lower the temperature used in DQMC, the larger the error bar is. In Fig. 7, we have simulated the system to the lowest temperature at our best while keep a reasonable error bar. The lowest temperature for the  $2 \times 75$  lattice is  $t/12$  and the lowest temperature for the  $2 \times 12$  lattice is  $t/15$ . Within our

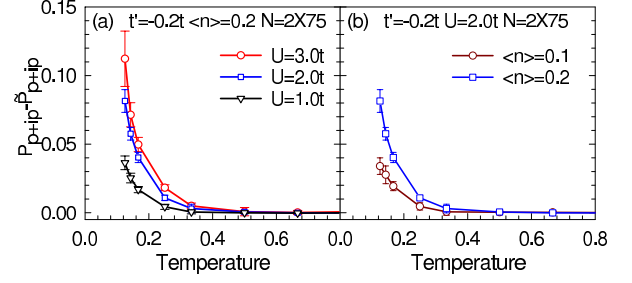


FIG. 8. (Color online) The intrinsic pairing interaction  $P_{p+ip} - \tilde{P}_{p+ip}$  as a function of temperature for different  $U$  (a) and different  $\langle n \rangle$  (b) on a  $2 \times 75$  lattice.

numerical results, We fit the DQMC data with a formula of  $P = a/(T - T_c) + b$ , as shown (dashed lines) in Fig. 7 and then we extrapolate to obtain the superconducting transition temperature  $T_c$ . The fitting agrees with the DQMC data reasonably well. From this fitting, one may estimate a  $T_c$  of about  $\sim 0.01t$ , which is roughly  $\sim 200K$ .

In order to extract the intrinsic pairing interaction in our finite system, one should subtract from  $P_\alpha$  its uncorrelated single-particle contribution  $\tilde{P}_\alpha$ , which is achieved by replacing  $\langle c_{i\downarrow}^\dagger c_{j\downarrow} c_{i+\delta_l\uparrow}^\dagger c_{j+\delta_l'\uparrow} \rangle$  in Eq. (4) with  $\langle c_{i\downarrow}^\dagger c_{j\downarrow} \rangle \langle c_{i+\delta_l\uparrow}^\dagger c_{j+\delta_l'\uparrow} \rangle$ . Clearly in Fig. 8, the intrinsic pairing interaction  $P_{p+ip} - \tilde{P}_{p+ip}$  shows qualitatively the same temperature dependence as that of  $P_{p+ip}$ , which is positive and increases with the lowering of temperature. Such a temperature dependence of  $P_\alpha - \tilde{P}_\alpha$  suggests effective attractions generated between electrons and the instability toward SC in the system at low temperatures. Moreover, Fig. 8(a) shows that the intrinsic pairing interaction for  $p + ip$  symmetry enhances with larger  $U$ , indicating the enhanced pairing strength with the enhancement of the electron correlations. As for the other two pairing symmetries shown, our DQMC results yield negative intrinsic pairing interactions, reflecting the fact that the realization of the  $p + ip$  symmetry at low temperatures will suppress other competing pairing channels.

**Conclusions and discussions:** We have performed RPA analysis for the honeycomb Hubbard model with weak repulsive  $U$  interactions and DQMC calculations for intermediate interactions at low electron filling where the DOS is parametrically large. Both studies shows that the triplet  $p + ip$  SC occurs as the ground state of our model system of low-filled graphene. Besides graphene, by trapping some fermionic cold atoms into an optical lattice, one may also be able to simulate the Hubbard-model on a honeycomb lattice studied here[26–28], which is expected to realize an exotic triplet  $p + ip$  superfluidity.

*Acknowledgement:* We would like to thank Zhong-Bin Huang, Yuigui Yao, Yu-Zhong Zhang, and Su-Peng Kou for stimulating discussions. This work is supported in part by NSCF (Grant Nos. 11104014, 11274041, 11374034, and 11334012), by Research Fund

for the Doctoral Program of Higher Education of China 20110003120007 and SRF for ROCS (SEM) (T.M.), by the NCET program under the grant No. NCET-12-0038 (F.Y.), and by the Thousand-Young-Talent Program of China (H.Y.).

---

\* yangfan\_blg@bit.edu.cn

† yaohong@tsinghua.edu.cn

- [1] K.S. Novoselov, A. K. Geim, S. V. Morozov, D. Jiang, Y. Zhang, S. V. Dubonos, I. V. Gregorieva, and A. A. Firsov, *Science* **306**, 666 (2004).
- [2] For a review, see A. H. Castro Neto, F. Guinea, N. M. R. Peres, K. S. Novoselov and A. K. Geim, *Rev. Mod. Phys.* **81**, 109 (2009).
- [3] S. Raghu, S. A. Kivelson, and D. J. Scalapino, *Phys. Rev. B* **81**, 224505 (2010).
- [4] R. Nandkishore, L. S. Levitov, and A. V. Chubukov, *Nat. Phys.* **8**, 158 (2012).
- [5] W.-S. Wang, Y.-Y. Xiang, Q.-H. Wang, F. Wang, F. Yang, and D.-H. Lee, *Phys. Rev. B* **85**, 035414 (2012).
- [6] M. L. Kiesel, C. Platt, W. Hanke, D. A. Abanin, and R. Thomale, *Phys. Rev. B* **86**, 020507(R) (2012).
- [7] A. M. Black-Schaffer, S. Doniach, *Phys. Rev. B* **75**, 134512 (2007).
- [8] J. González, *Phys. Rev. B* **78**, 205431 (2008).
- [9] S. Pathak, V. B. Shenoy, G. Baskaran, *Phys. Rev. B* **81**, 085431 (2010).
- [10] X.-L. Qi and S.-C. Zhang, *Rev. Mod. Phys.* **83**, 1057 (2011).
- [11] M. Z. Hasan and C. L. Kane, *Rev. Mod. Phys.* **82**, 3045 (2010).
- [12] T. Li, arXiv:1103.2420 (2011).
- [13] I. Martin and C. D. Batista, *Phys. Rev. Lett.* **101**, 156402 (2008).
- [14] H. Yao and F. Yang, arXiv:1312.0077.
- [15] X. Chen, F. Yang, H. Yao, Y. Yao, and J. Ni, in preparation (2013).
- [16] S. Reich, J. Maultzsch, C. Thomsen, and P. Ordejón, *Phys. Rev. B* **66**, 035412 (2002).
- [17] T. Ma, F. M. Hu, Z. B. Huang, and H. Q. Lin, *Appl. Phys. Lett.* **97**, 112504 (2010).
- [18] N. E. Bickers, D. J. Scalapino, and S. R. White, *Phys. Rev. Lett.* **62**, 961 (1989).
- [19] D. J. Scalapino, *Rev. Mod. Phys.* **84**, 1383 (2012).
- [20] T. Takimoto, T. Hotta, and K. Ueda, *Phys. Rev. B* **69**, 104504 (2004); K. Yada and H. Kontani, *J. Phys. Soc. Jpn.* **74**, 2161 (2005).
- [21] K. Kubo, *Phys. Rev. B* **75**, 224509 (2007); K. Kuroki, S. Onari, R. Arita, H. Usui, Y. Tanaka, H. Kontani, and H. Aoki, *Phys. Rev. Lett.* **101**, 087004 (2008).
- [22] S. Graser, T. A. Maier, P. J. Hirschfeld, and D. J. Scalapino, *New Journal of Physics* **11**, 025016 (2009).
- [23] F. Liu, C.-C. Liu, K. Wu, F. Yang, and Y. Yao, *Phys. Rev. Lett.* **111**, 066804 (2013); L.-D. Zhang, F. Yang and Y. Yao, arXiv:1309.7347
- [24] R. Blankenbecler, D. J. Scalapino, and R. L. Sugar, *Phys. Rev. D* **24**, 2278 (1981).
- [25] T. Ma, F. M. Hu, Z. B. Huang, and H.-Q. Lin, *Horizons in World Physics*, **276**, Chapter 8, Nova Science Publishers, Inc, 2011.
- [26] S.-L. Zhu, B.G. Wang, and L.-M. Duan, *Phys. Rev. Lett.* **99**, 260402 (2007).
- [27] C. J. Wu, D. Bergman, L. Balents, and S. Das Sarma, *Phys. Rev. Lett.* **99**, 070401 (2007).
- [28] L. Tarruell, D. Greif, T. Uehlinger, G. Jotzu, and T. Esslinger, *Nature* **483**, 302 (2012).